Supplementary Materials of "Decentralized Dispatch of Distributed Multi-Energy Systems with Comprehensive Regulation of Heat Transport in District Heating Networks"

Qinghan Sun, *Student Member, IEEE*, Tian Zhao, Qun Chen, *Member, IEEE*, Kelun He, Huan Ma

This file includes the supplementary materials for the paper "Decentralized Dispatch of Distributed Multi-Energy Systems with Comprehensive Regulation of Heat Transport in District Heating Networks". Besides, the prior conference version is also attached to the end of the file.

I. Proof of Eqs. (8)-(11)

In the paper, we have shown that when fluid flow rates are constants, then the pipeline flow has the following closed-form solution:

$$\theta_{out}(t) = \theta_{in}(t-t_d)e^{-\frac{UL}{\dot{m}c_p}} \tag{1}$$

When mass flow rates vary at $t=0$, the fluid microelement that enters the pipeline at $t_{in} \geq 0$ will flow out after $t_{in}+t_d$. Therefore, we have:

$$\theta_{out}\left(t\right) = \theta_{in}\left(t-t_d\right)e^{-\frac{UL}{\dot{m}c_p}}, \quad t \geq t_d \tag{2}$$

The fluid microelement that flow out between $t=0$ and $t=t_d$ will encounter a sudden changes in the pipeline. In this case, the microelement can be considered as successively entering two pipelines with different lengths at rates of $\dot{m}^{his}$ and $\dot{m}$ respectively. The length of the first pipeline is $L_1 = L - \frac{\dot{m}t}{\rho A}$ and that of the second pipeline is $L_2 = \frac{\dot{m}t}{\rho A}$. Therefore, we obtain:

$$\theta_{out}\left(t\right) = \theta_{in}^{his}\left(t-t_{d,1}-t_{d,2}\right)e^{-\frac{UL_1}{\dot{m}^{his}c_p}}e^{-\frac{UL_2}{\dot{m}c_p}}, \quad t \leq t_d \tag{3}$$

where $t_{d,1} = \frac{L_1}{\dot{m}^{his}/\rho A}$ and $t_{d,2} = t$ are the delay time of the two pipelines. Noting that $t - t_{d,1} - t_{d,2} \leq 0$, we have change the label of inlet temperature curve from θ_{in} to θ_{in}^{his}. Reorganize (3) so that it has a form similar to (2), and we then obtain:

$$\theta_{out}\left(t\right) = \begin{cases} \theta_{in}\left(t-t_d\right)e^{-\frac{UL}{\dot{m}c_p}} & t \geq t_d \\ \theta_{in}^{his}\left(\frac{\dot{m}}{\dot{m}^{his}}\left(t-t_d\right)\right)e^{-\frac{UL}{\dot{m}c_p}+a(t-t_d)} & t \leq t_d \end{cases}$$

$$a = \frac{-U}{\rho A c_p}\left(1-\frac{\dot{m}}{\dot{m}^{his}}\right) \tag{4}$$

Define an auxiliary function θ_{in}^{ext} be the extended inlet temperature:

$$\theta_{in}^{ext}\left(t\right) = \begin{cases} \theta_{in}^{his}\left(\frac{\dot{m}}{\dot{m}_{his}}t\right)e^{at} & t \leq 0 \\ \theta_{in}\left(t\right) & t \geq 0 \end{cases} \tag{5}$$

Let $\Theta_{in}^{his}[i] = \theta_{in}^{his}(i\Delta t)$ with $i \in \{-M_{his}, ..., -1\}$ be the discrete sampling of historical temperature data $\theta_{in}^{his}(t)$, and $\Theta_{in}^{ext}[i] = \theta_{in}^{ext}(i\Delta t)$ with $i \in \{-M_{his}, ..., -1, 0, ..., M-1\}$ be the sampling of the extended inlet temperature function. Then, it can be obtained that

$$\begin{aligned} \Theta_{in}^{ext}[i] &= \sum_{k=0}^{\frac{M}{2}} \widetilde{\Theta}_{in}^{ext}[k]\cos k\omega i + \sum_{k=1}^{\frac{M}{2}-1} \widetilde{\Theta}_{in}^{ext}[k+\frac{M}{2}]\sin k\omega i \\ &= \theta_{in}^{ext}(i\Delta t) = \theta_{in}^{his}\left(\frac{\dot{m}}{\dot{m}_{his}}i\Delta t\right)e^{ai\Delta t} \\ &= \left(\sum_{k=0}^{\frac{M}{2}} \widetilde{\Theta}_{in}^{his}[k]\cos k\omega\left(\frac{\dot{m}}{\dot{m}_{his}}i\right)\right. \\ &\left. + \sum_{k=1}^{\frac{M}{2}-1} \widetilde{\Theta}_{in}^{his}[k+\frac{M}{2}]\sin k\omega\left(\frac{\dot{m}}{\dot{m}_{his}}i\right)\right)e^{ai\Delta t} \\ &\text{when } i \in \{-M_{his}, ..., -1\} \end{aligned} \tag{6}$$

Combined with that $\Theta_{in}^{ext}[i] = \Theta_{in}[i]$ for $i \in \{0, ..., M-1\}$, we have:

$$\Theta_{in}^{ext} = \begin{bmatrix} \mathbf{L}_s\mathbf{L}_d\widetilde{\Theta}_{in}^{his} \\ \Theta_{in} \end{bmatrix} \tag{7}$$

where,

$$\mathbf{L}_s = diag\left(e^{(-M_{his})a\Delta t}, e^{(-M_{his}+1)a\Delta t}, ..., e^{(-1)a\Delta t}\right)$$

$$\mathbf{L}_{d,ij} = \begin{cases} \cos\frac{\dot{m}}{\dot{m}^{his}}\omega\left(i-M_{his}\right)j & j = 0, ..., \frac{M_{his}}{2} \\ \sin\frac{\dot{m}}{\dot{m}^{his}}\omega\left(i-M_{his}\right)\left(j-\frac{M_{his}}{2}\right) & j = \frac{M_{his}}{2}+1, ..., M_{his}-1 \end{cases}$$
$$i = 0, ..., M_{his}-1 \tag{8}$$

Noting that,

$$\theta_{out}\left(t\right) = \theta_{in}^{ext}\left(t-t_d\right)e^{-\frac{UL}{\dot{m}c_p}} \tag{9}$$

Therefore, similar to (5) in the main manuscript, we obtain:

$$\Theta_{out} = \begin{bmatrix} \mathbf{0}_{M_{his}\times M} \\ \mathbf{I}_M \end{bmatrix}^T \mathbf{A'B'A'}^{-1} \begin{bmatrix} \mathbf{L}_s\mathbf{L}_d\widetilde{\Theta}_{in}^{his} \\ \Theta_{in} \end{bmatrix} \tag{10}$$

It is worth noting that the converting matrix $\mathbf{A'B'A'}^{-1}$ is pre-multiplied by an extra $[\mathbf{0}_{M\times M_{his}} \ \ \mathbf{I}_M]$ to take the last M rows. This is because we only concern the decisions for $t \geq 0$, i.e., $i \in \{0, ..., M-1\}$.

If we partition $\mathbf{A'B'A'}^{-1}$ into block forms:

$$\mathbf{A'B'A'}^{-1} = \begin{bmatrix} \mathbf{K}_{M_{his}\times M_{his}}^{11} & \mathbf{K}_{M_{his}\times M}^{12} \\ \mathbf{K}_{M\times M_{his}}^{21} & \mathbf{K}_{M\times M}^{22} \end{bmatrix} \tag{11}$$

(10) can be further reduced to:

$$\boldsymbol{\theta}_{out} = \mathbf{K}^{21}_{M\times M_{his}}\mathbf{L}_s\mathbf{L}_d\widetilde{\boldsymbol{\theta}}^{his}_{in} + \mathbf{K}^{22}_{M\times M}\boldsymbol{\theta}_{in} \tag{12}$$

Recalling that $\widetilde{\boldsymbol{\theta}}^{his}_{in}$ and $\boldsymbol{\theta}^{his}_{in}$ are related by a trigonometric interpolation matrix, which we denote as $\mathbf{A}^{his}$. Then we get,

$$\begin{aligned}
&\boldsymbol{\theta}_{out} = \mathbf{C}_{his}\left(\dot{m}\right)\boldsymbol{\theta}^{his}_{in} + \mathbf{C}_{cur}\left(\dot{m}\right)\boldsymbol{\theta}_{in}\\
&\mathbf{C}_{his}\left(\dot{m}\right) = \mathbf{K}^{21}_{M\times M_{his}}\mathbf{L}_s\mathbf{L}_d\left(\mathbf{A}^{his}\right)^{-1}\\
&\mathbf{C}_{cur}\left(\dot{m}\right) = \mathbf{K}^{22}_{M\times M_{his}}
\end{aligned} \tag{13}$$

Noting that the pipelines exhibit storage capabilities, which should be also considered just like a conventional storage device. For any pipeline, the accumulated heat storage variation over the dispatch period should be zero.

$$\int_{t=0}^{t_{end}}\frac{\mathrm{d}H_{sto}}{\mathrm{d}t}dt = \int_{t=0}^{t_{end}}(\Phi_{ij,in} - \Phi_{ij,out} - \Phi_{ij,loss})dt = 0 \tag{14}$$

where $\Phi_{ij,in}$, $\Phi_{ij,out}$ and $\Phi_{ij,loss}$ are the enthalpy flow rate at the inlet and outlet, and the heat losses.

$$\Phi_{ij,in} = \dot{m}c_pT_{ij,in} \tag{15}$$

$$\Phi_{ij,out} = \dot{m}c_pT_{ij,out} \tag{16}$$

For simplicity, the losses are estimated as:

$$\int_{t=0}^{t_{end}}\Phi_{ij,loss}dt \approx \int_{t=0}^{t_{end}}\dot{m}c_p\theta_{ij,in}e^{-\frac{UL}{\dot{m}c_p}}dt \tag{17}$$

and (14) is then reduced to:

$$\begin{aligned}
\int_{t=0}^{t_{end}}\frac{\mathrm{d}H_{sto}}{\mathrm{d}t}dt &= \int_{t=0}^{t_{end}}(\Phi_{ij,in} - \Phi_{ij,out} - \Phi_{ij,loss})dt\\
&\approx \int_{t=0}^{t_{end}}\dot{m}c_p\left(\theta_{ij,in}e^{-\frac{U_{ij}L_{ij}}{\dot{m}_{ij}c_p}} - \theta_{ij,out}\right)dt = 0
\end{aligned} \tag{18}$$

(4), (10), (13) and (18) are exactly (8)-(11) in the main body of the manuscript.

II. Mathematical Expressions of the Thermal Resistancess

In (36) and (37), we involve the thermal resistances of the HES and the radiator, whose expressions are [1],

$$R^{\mathrm{HES}}_{i,t} = \frac{\dot{m}_ic_pe^{\frac{kA^{\mathrm{SHN,HES}}_i}{\dot{m}^{\mathrm{SHN,HES}}_{i,t}c_p}} - \dot{m}^{\mathrm{HES}}_{i,t}c_pe^{\frac{kA^{\mathrm{HES}}_i}{\dot{m}_ic_p}}}{\dot{m}_ic_p\dot{m}^{\mathrm{SHN,HES}}_{i,t}c_p\left(e^{\frac{kA^{\mathrm{HES}}_i}{\dot{m}^{\mathrm{SHN,HES}}_{i,t}c_p}} - e^{\frac{kA^{\mathrm{HES}}_i}{\dot{m}_ic_p}}\right)} \tag{19}$$

$$R^{\mathrm{RAD}}_{i,t} = \frac{1}{\dot{m}^{\mathrm{RAD}}_{i,t}c_p\left(1 - e^{-\frac{kA^{\mathrm{RAD}}_i}{\dot{m}^{\mathrm{RAD}}_{i,t}c_p}}\right)} \tag{20}$$

where kA is the heat transfer coefficient multiplied by the area of the HES and the radiator.

III. Explanation of Algorithm 2

In the manuscript, we have compacted the dispatch problem, presented the partial augmented lagrangian $L\left(\mathbf{X},\mathbf{Y},\boldsymbol{\lambda}\right)$ and the optimal dual objective $\xi\left(\mathbf{Y}\right)$. We want to minimize $\xi\left(\mathbf{Y}\right)$ over $\mathbf{Y}\in\mathcal{H}$. We define $\xi^{(k)}$ as the estimation of $\xi\left(\mathbf{Y}\right)$ given by ADMM at kth iteration

$$\begin{aligned}
\xi^{(k)} &\triangleq \xi\left(\mathbf{Y}'^{(k)}\right) \approx L\left(\mathbf{X}^{(k+1)},\mathbf{Y}'^{(k)},\boldsymbol{\lambda}'^{(k+1)}\right)\\
&= \sum_{i=1}^{N}L_i^{(k)} = \sum_{i=1}^{N}L_i\left(\mathbf{X}_i^{(k+1)},\mathbf{Y}_i'^{(k)},\boldsymbol{\lambda}_i'^{(k+1)}\right)
\end{aligned} \tag{21}$$

Recalling that in the paper we have selected $\dot{m}_i, i\neq l_0$ as independent decision variables and the gradients c_i can be calculated through

$$\begin{aligned}
c_i &\triangleq \frac{\partial\xi^{(k)}}{\partial\dot{m}_i'^{(k)}}\\
&= \sum_{j=l_0}^{l_{N_h}-1}\left(\frac{\partial L_j^{(k)}}{\partial\mathbf{Y}_j'^{(k)}} + \boldsymbol{\mu}^{(k)T}_{\mathbf{A}_j}\frac{\partial\mathbf{A}_j^{(k)}}{\partial\mathbf{Y}_j'^{(k)}}\right)\frac{\partial\mathbf{Y}_j'^{(k)}}{\partial\dot{m}_i'^{(k)}}\\
&= \sum_{j=l_0}^{l_{N_h}-1}\frac{\partial\xi_j^{(k)}}{\partial\mathbf{Y}_j'^{(k)}}\frac{\partial\mathbf{Y}_j'^{(k)}}{\partial\dot{m}_i'^{(k)}}
\end{aligned} \tag{22}$$

We will then show how the decentralized gradient calculation and decentralized step size calculation processes in **Algorithm 2** are designed.

A. Decentralized Gradient Calculation

We first expand (22) to,

$$\begin{aligned}
c_i &= \sum_{j=l_0}^{l_{N_h}-1}\frac{\partial\xi_j^{(k)}}{\partial\mathbf{Y}_j'^{(k)}}\frac{\partial\mathbf{Y}_j'^{(k)}}{\partial\dot{m}_i'^{(k)}}\\
&= \sum_{j=l_0}^{l_{N_h}-1}\left(\frac{\partial\xi_j^{(k)}}{\partial\dot{m}_j'^{(k)}}\frac{\partial\dot{m}_j'^{(k)}}{\partial\dot{m}_i'^{(k)}} + \sum_{v\in\mathcal{N}_j^h}\frac{\partial\xi_j^{(k)}}{\partial\dot{m}_{jv}'^{(k)}}\frac{\partial\dot{m}_{jv}'^{(k)}}{\partial\dot{m}_i'^{(k)}}\right)
\end{aligned} \tag{23}$$

It is obvious that, $\frac{\partial\dot{m}_j'^{(k)}}{\partial\dot{m}_i'^{(k)}} = 0$ for $\forall j\neq l_0$ and $j\neq i$ since they are independent, and that $\frac{\partial\dot{m}_{jv}'^{(k)}}{\partial\dot{m}_i'^{(k)}}$ can only take 0 or ±1 according to mass conservation.

Since we assumed that the PHN is a connected radial one composed of symmetric pipelines, there is a unique path connecting the DES node i and the slack node l_0, as illustrated by the red lines in Fig. 1. If $\dot{m}_i$ is adjusted, only the fluid flow rates along the red path will be affected. Applying mass conservation along the path, we then obtain,

$$\frac{\partial\dot{m}_{u_xx}'^{(k)}}{\partial\dot{m}_i'^{(k)}} = \begin{cases}-b_{u_xx}t_i & u_xx \text{ is on the path from } i \text{ to } l_0\\ 0 & \text{otherwise}\end{cases} \tag{24}$$

$$\frac{\partial\dot{m}_{l_0}'^{(k)}}{\partial\dot{m}_i'^{(k)}} = -t_{l_0}t_i \tag{25}$$

Therefore, (23) can be further reorganized to:

$$\begin{aligned}
c_i =& \frac{\partial\xi_i^{(k)}}{\partial\dot{m}_i'^{(k)}} - t_i\left[t_{l_0}\frac{\partial\xi_{l_0}^{(k)}}{\partial\dot{m}_{l_0}'^{(k)}}\right.\\
&\left. + \sum_{\substack{u_jj \text{ on}\\ \text{the path}}}\left(b_{u_jj}\frac{\partial\xi_j^{(k)}}{\partial\dot{m}_{u_jj}'^{(k)}} + b_{u_jj}\frac{\partial\xi_{u_j}^{(k)}}{\partial\dot{m}_{u_jj}'^{(k)}}\right)\right]\\
=& \frac{\partial\xi_i^{(k)}}{\partial\dot{m}_i'^{(k)}} - t_ia_i
\end{aligned} \tag{26}$$

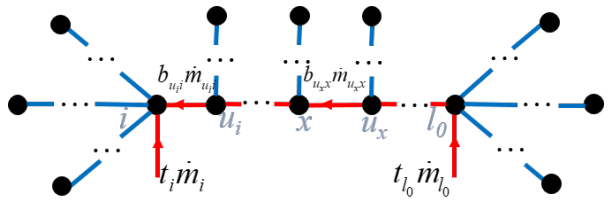

Fig. 1. The sketch of a connected radial PHN network. Due to symmetry, we only present the supply pipelines. u_i denotes the first node on the path towards l_0. $t_i = 1$ if DES node i is a HS node and $t_i = -1$ if node i is a HC node. $b_{ij} = 1$ if fluid flows from i to j and $b_{ij} = -1$ indicates the opposite case.

where we have denote the term in the square brackets as a_i. a_i and a_{u_i} reveal the following relationship,

$$a_i = \underbrace{a_{u_i} + b_{u_i i}\frac{\partial \xi_{u_i}^{(k)}}{\partial \dot{m}_{u_i i}^{\prime(k)}}}_{a_{u_i i}} + b_{u_i i}\frac{\partial \xi_i^{(k)}}{\partial \dot{m}_{u_i i}^{\prime(k)}} \tag{27}$$

The terms a_i and $a_{u_i i}$ are exactly the auxiliary variables in **Algorithm 2**, which are shared between nodes and calculated in a recursive manner.

B. Decentralized Step Size Calculation

In the step size calculation part of **Algorithm 2**, each DES node in the PHN will first wait for d_{ij} and $s_{ij}^{\max}$ from all neighbouring nodes except u_i.

$s_{ij}^{\max}$ is the maximum step size summarized by node j and its child nodes. Herein, the 'child nodes' refer to all the nodes still connected to j when pipeline $u_j j$ is broken. In step 16 of **Algorithm 2**, the DES node will calculate the maximum local step size, and compare it to $s_{ij}^{\max}$ to obtain the minimal one.

The physical meaning of auxiliary variables d_{ij} is a bit tricky. A intuitive explanation is that, if we adjust the fluid flow rates of node j and its child nodes along the descent direction with step size s, $\dot{m}_{ij}$ will also vary, and such variation should be sd_{ij}. Such definition inspires step 19 and 20 in **Algorithm 2**. Step 19 calculates $d_{u_i i}$ and the formula employed can be obtained by applying mass conservation to DES node i,

$$b_{u_i i}\dot{m}_{u_i i} + t_i\dot{m}_i = \sum_{j\in\mathcal{N}_i^h j\neq u_i} b_{ij}\dot{m}_{ij} \tag{28}$$

According to the definition of d, the above equation still holds after gradient descent with a step of s, which gives,

$$b_{u_i i}sd_{u_i i} + t_i(-sc_i) = \sum_{j\in\mathcal{N}_i^h j\neq u_i} b_{ij}sd_{ij} \tag{29}$$

which directly leads to the formula in step 19. Step 20 further calculates the maximum step size considering box constraints of $\dot{m}_{u_i i}$.

Finally, all the candidate step sizes are gathered by the slack node l_0 to determine the eventual step size s.

IV. Performance of Directly Applying ADMM

Fig. 2 displays the convergence trajectories of ADMM. The decision variables oscillate significantly. Such oscillations are inferred to result from the bilinear terms in the constraints.

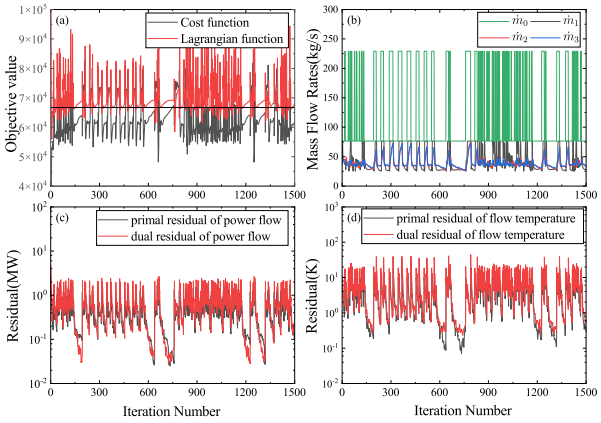

Fig. 2. The convergence curves given by the direct application of ADMM. A relaxing factor of 0.5 is used. Besides, the objective function further include the proximal terms, i.e. $\frac{\gamma}{2}\|\mathbf{X}_i - \mathbf{X}_i^{(k)}\|^2$ and $\frac{\gamma}{2}\|\mathbf{Y}_i - \mathbf{Y}_i^{(k)}\|^2$, where $\gamma = 10$

References

[1] J. Hao, Q. Chen, K. He, L. Chen, Y. Dai, F. Xu, and Y. Min, "A heat current model for heat transfer/storage systems and its application in integrated analysis and optimization with power systems," *IEEE Trans. Sustain. Energy*, vol. 11, no. 1, pp. 175–184, 2020.

Fully Decentralized Dispatch of Integrated Power Distribution and Heating Systems Considering Nonlinear Heat Transfer Processes

Qinghan Sun, Qun Chen, Kelun He
Department of Engineering Mechanics, Tsinghua University
Beijing, China
sqh20@mails.tsinghua.edu.cn, chenqun@tsinghua.edu.cn, hekl@mail.tsinghua.edu.cn

***Abstract*—Decentralized dispatch of distributed energy systems connected with distribution networks(DN) and district heating systems(DHS) has drawn great attention recently. However, the heat transfer between fluids with different temperatures in the heating system usually lacks proper consideration. In this work, the delay and loss characteristics of the pipelines and the heat transfer at the heat exchange stations in the DHS are thoroughly modelled. A fully decentralized solution based on Alternating Direction Method of Multipliers(ADMM) is used to solve the dispatch problem. Case study on a integrated system composed of 17 agents validates the importance of a comprehensive DHS model and the effectiveness of the proposed method.**

***Index Terms*—Decentralized Dispatch, Distributed Energy Systems(DES), District Heating Systems(DHS), Alternating Direction Method of Multipliers(ADMM)**

I. Introduction

With increasing concerns on a low carbon energy structure, distributed energy systems(DES) with sophisticated management schemes have drawn increasing attention. A DES usually consists of residential wind and solar power, micro gas turbines and heat pumps, which diversify generation processes and are more resilient to demand fluctuations. Therefore, on-site DESs have great potentials to reduce transmission losses and increase renewable energy penetration [1]. Furthermore, networked DESs can improve energy supplying reliability and promote user-side energy utilization efficiency through synergy between multi-energy flows.

In order to coordinate multi-agent DESs, a centralized system operator can be appointed to collect their information and make dispatch decisions. However, the DESs are owned by different agents and thus reveal a decentralized nature. This makes coordination through a centralized dispatch operator impractical. Therefore, decentralized schemes are developed, where each agent shares limited information with neighbours and participates in the optimization. Compared to centralized optimization, decentralized schemes protect individual privacy [2], enable parallel calculation and improve solution robustness in case of single-point failure [3].

Typical decentralized algorithms include dual decomposition method [4], alternating direction method of multipliers(ADMM) [5], and optimality condition decomposition methods [6], which split the optimization problem into several subproblems and solve them iteratively. So far, these methods have been widely applied to the coordination of multiple DESs connected with distribution networks(DN), and ADMM has been extensively popular due to its convenience for application. Nevertheless, in terms of multi-energy systems with district heating systems(DHS), researches mainly focus on the energy-carrier-based decentralization. For instance, in [7] and [8], the decentralization agents are operators of the DN and DHS, and the combined heat and power sources only serve as coupling devices whose control authority is shared between the two operators. This is vastly different from the decentralization in DN and the privacy of DES owners is not fully preserved.

A few researches have also made node-level decentralization attempts based on DES agents in multi-energy systems. However, the DHS usually lacks proper consideration of heat transfer processes due to high nonlinearity. Reference [9] performs energy-hub based decentralized operation of multi-energy systems, while the delay of flow and the heat transfer constraints are dismissed. In [10], a dispatching framework is estabilished among several interconnected regions. Still heat transfer constraints are not considered, and therefore the flow temperatures in the DHS might not be precisely estimated and the decisions may turn out unreasonable. Actually, the heat transport in DHS consists of both heat migration accompanying with fluid flows and heat transfer between fluids with different temperatures, which should be thoroughly considered. Besides, the physical nature also implies the delay and storage characteristics of heating networks, which have the potentials to be exploited to further promote accommodation of the renewables and reduce carbon emissions [11].

Therefore, this work aims to characterize the DHS more comprehensively and employ a fully decentralized optimization scheme of DESs connected with integrated power distribution and heating systems. The heat current method [12] embedding nonlinearity into linear heat circuits is used to describe the heat transfer process. The remainder of this article is organized as follows: Section II describes the model of multiple DES with DN and DHS. Section III proposes the ADMM-based fully decentralized solution. Section IV presents case study on an integrated system composed of a 14-node heating network and a 14-bus power distribution system.

The present work is supported by the National Natural Science Foundation of China (Grant Nos. 51836004 and 52125604)

II. Mathematical Model of Networked DESs

Fig. 1(a) reveals the sketch of a DES, which is implemented with micro-turbine-based combined heat and power(CHP) systems, photovoltaic(PV) panels, wind turbines(WT) and heat pumps(HP). The DES can exchange power with the distribution network(DN) to maintain power balance. Besides, the heating devices in the system are connected through a secondary heating network(SHN), which can exchange heat with the primary heating network(PHN) through a heat exchange station(HES). The SHN and PHN constitute the self-sufficient DHS. The DESs can either work in heat source(HS) or heat customer(HC) modes. In the HC mode(Fig. 1(a)), local devices and the PHN work together to meet the heat demand of end users. In the HS mode(Fig. 1(b)), The DES works reversely as a heat source of the PHN. Fig. 1.(c) shows the structure of networked DESs connected through the DN and PHN. The DESs can connect to one or both of the networks.

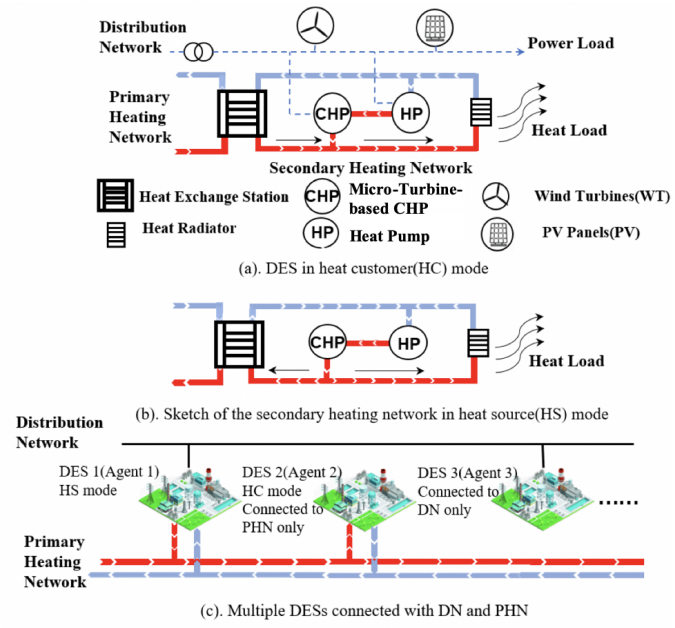

Fig. 1. The sketch of DESs. The mass flow direction in (a) and (b) are different. In (a) the PHN and local devices together provide heat to the local customer. In (b), local devices in turn provide heat to the PHN.

A. Modelling of DN

The DN is a radial network, which can be abstracted as a tree shown in Fig. 2. Each node represents a DES agent. The DN connects the upper-level grid at node 0, whose voltage is nominal value 1. The father node of node i is labelled as A_i, and the set of child nodes is $\mathbf{C}_i$. According to second-order-cone relaxed distflow model [13], the constraints are:

$$P_{i,t} = P'_{i,t} - l_{i,t}R_{A_i i} = \sum_{j\in\mathbf{C_i}} P'_{j,t} + P_{l,i,t} \tag{1}$$

$$Q_{i,t} = Q'_{i,t} - l_{i,t}X_{A_i i} = \sum_{j\in\mathbf{C_i}} Q'_{j,t} + Q_{l,i,t} \tag{2}$$

$$v_{A_i,t} = v_{i,t} + 2\left(R_{A_i i}P'_{i,t} + X_{A_i i}Q'_{i,t}\right) - l_{i,t}\left(R^2_{A_i i} + X^2_{A_i i}\right) \tag{3}$$

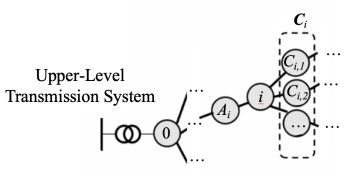

Fig. 2. Tree topology of radial distribution networks

$$v_{A_i,t}l_{i,t} \geq P'^2_{i,t} + Q'^2_{i,t} \tag{4}$$

$$\underline{v} \leq v_{i,t} \leq \overline{v} \tag{5}$$

$$P^2_{i,t}{}' + Q^2_{i,t}{}' \leq S_i^{max\ 2} \tag{6}$$

where P and Q represent the active and reactive power. v and l denote the squared magnitude of nodal voltage and transmission line current. $P_{i,t}$ and $Q_{i,t}$ represent transmission line power from A_i to i and $P'_{i,t}(Q'_{i,t})$ include transmission losses. $\underline{v}$, $\overline{v}$ and S_i^{max} are voltage and apparent power limits.

B. Modelling of PHN

As revealed in Fig. 1(c), the PHN can be seen as a set of DES nodes connected parallelly with symmetric supply and return pipelines. Each node consists of a pair of junctions and a HES to exchange heat with the PHN.

1) Pipelines: Typically, the PHN is operated at "quality regulation" mode with constant pipeline mass flow rate, because frequent adjustment of flow rate may induce hydraulic imbalances. Considering delay and heat loss, the relationship between inlet and outlet temperature of each pipeline can be described through the node method in [7]:

$$T^{out}_{ij,t} = \left(T^{in}_{ij,t-\Delta t_{ij}} - T_a\right) e^{-\frac{U_{ij}L_{ij}}{\dot{m}_{ij}c_p}} + T_a \tag{7}$$

$$\Delta t_{ij} = \frac{L_{ij}\rho_w A_{ij}}{\dot{m}_{ij}\tau} \tag{8}$$

where the subscript ij represent the pipeline connecting node i and j, and the superscripts in and out discriminates the pipeline inlet and outlet. U_{ij} is the coefficient of thermal conductivity. L_{ij} and A_{ij} are the pipeline length and cross-section area, respectively. $\dot{m}_{ij}$ is the mass flow rate and c_p is the heat capacity of water flow. T_a is the ambient temperature. Δt_{ij} denotes the dimensionless delay time and τ represents the time interval of dispatch. Note that $\Delta t - t_{ij}$ may not be interger according to (8). In this situation, $T^{in}_{ij,t-\Delta t_{ij}}$ is calculated using inlet flow temperatures at adjacent interger time sections.

$$T^{in}_{ij,t-\Delta t_{ij}} = \gamma T^{in}_{ij,\lceil t-\Delta t_{ij}\rceil} + (1-\gamma)\, T^{in}_{ij,\lfloor t-\Delta t_{ij}\rfloor} \tag{9}$$

$$\gamma = \lceil t - \Delta t_{ij}\rceil - (t - \Delta t_{ij}) \tag{10}$$

2) Pipeline junctions: At the junctions of pipelines, the net mass flow rate is zero according to mass conservation.

$$\sum \dot{m}_{s,j\to i} = \sum \dot{m}_{s,i\to k} + \dot{m}_i \tag{11}$$

$$\sum \dot{m}_{r,k\to i} + \dot{m}_i = \sum \dot{m}_{r,i\to j} \tag{12}$$

where s and r are short for supply and return pipelines. $\dot{m}_i$ denotes the mass flow rate that enters HES i, which is positive for HES in HC modes and negative for HES in HS modes.

Besides, energy conservation gives the following constraints at the junctions:

HES in HC modes:

$$\sum \dot{m}_{s,j\to i} T^{out}_{ji,t} = T^{mix}_{s,i,t}\left(\sum \dot{m}_{s,i\to k} + \dot{m}_i\right) \tag{13}$$

$$\sum \dot{m}_{r,k\to i} T^{out}_{ki,t} + \dot{m}_i T^{PHN}_{r,i,t} = T^{mix}_{r,i,t} \sum \dot{m}_{r,i\to j} \tag{14}$$

HES in HS modes:

$$\sum \dot{m}_{s,j\to i} T^{out}_{ji,t} + |\dot{m}_i| T^{PHN}_{s,i,t} = T^{mix}_{s,i,t} \sum \dot{m}_{s,i\to k} \tag{15}$$

$$\sum \dot{m}_{r,k\to i} T^{out}_{ki,t} = T^{mix}_{r,i,t}\left(\sum \dot{m}_{r,i\to j} + |\dot{m}_i|\right) \tag{16}$$

where $T^{mix}_{s,i,t}$ and $T^{mix}_{r,i,t}$ are mixed temperature at the junctions. $T^{PHN}_{s,i,t}$ and $T^{PHN}_{r,i,t}$ are the supply and return flow temperature at the primary side of HES i. $T^{mix}_{s,i,t} = T^{PHN}_{s,i,t}$ for HC nodes and $T^{mix}_{r,i,t} = T^{PHN}_{r,i,t}$ for HS nodes.

The heat exchange between the HES and PHN is,

$$H_{i,t} = \dot{m}_i c_p (T^{PHN}_{s,i,t} - T^{PHN}_{r,i,t}) \tag{17}$$

Apart from the above energy conservation equation, the heat transfer between fluids with different temperatures at the DESs should be further modelled, which will be explained comprehensively in section II-C.

C. Modelling of DESs

The DESs are prosumers of power and heat. Since the scale of a DES is usually small, we neglect the power flow constraints and SHN delay and losses. The power and heat balance equations are listed as follows:

$$P_{i,t} = P^l_{i,t} + P^{HP}_{i,t} - P^{CHP}_{i,t} - P^{WT}_{i,t} - P^{PV}_{i,t} \tag{18}$$

$$Q_{i,t} = Q^l_{i,t} - Q^{CHP}_{i,t} - Q^{WT}_{i,t} - Q^{PV}_{i,t} \tag{19}$$

$$H_{i,t} = H^l_{i,t} - H^{CHP}_{i,t} - H^{HP}_{i,t} \tag{20}$$

where superscript l denotes loads. The other terms with superscripts such as CHP and HP represent the generation of corresponding devices. The operation constraints are,

$$\underline{P^{CHP}_i} \le P^{CHP}_{i,t} \le \overline{P^{CHP}_i}, \quad Q^{CHP}_{i,t} = P^{CHP}_{i,t} \tan\theta_{CHP,i} \tag{21}$$

$$0 \le P^{WT}_i \le \overline{P^{WT}_i}, \quad Q^{WT}_{i,t} = P^{WT}_{i,t} \tan\theta_{WT,i} \tag{22}$$

$$0 \le P^{PV}_i \le \overline{P^{PV}_i}, \quad Q^{PV}_{i,t} = P^{PV}_{i,t} \tan\theta_{PV,i} \tag{23}$$

$$0 \le P^{HP}_i \le \overline{P^{HP}_i} \tag{24}$$

$$H^{CHP}_{i,t} = k_{CHP,i} P^{CHP}_{i,t} \tag{25}$$

$$H^{HP}_{i,t} = COP_{HP,i} P^{CHP}_{i,t} \tag{26}$$

where θs represent the power angles. $k_{CHP,i}$ is the heat-to-power ratio of CHP i and $COP_{HP,i}$ denotes the coefficient of performance of heat pump i.

The generation cost of the DES can be represented as:

$$C_{i,t} = f^{CHP}_i\left(P^{CHP}_{i,t}, H^{CHP}_{i,t}\right) \tag{27}$$

where $f(\cdot)$ is a quadratic funtion. Details can be found in [14].

As have been discussed, the heat transport from the PHN and heating devices to end users involves several heat transfer processes in the SHN. A nearly proposed heat current method [12] which provides an analogy to linear electrical circuits can be used to characterize them.

1) Heat current model of HC nodes: The heat current model of the SHN in HC mode is presented in Fig. 3(a). The constraints are:

$$T^{PHN}_{s,i,t} - T^{SHN}_{r,i,t} = R^{HES}_{i,t} H_{i,t} \tag{28}$$

$$T^{SHN}_{s,i,t} - T_{room} = R^{RAD}_{i,t} H^l_{i,t} \tag{29}$$

$$\dot{m}^{RAD}_{i,t} c_p (\epsilon^{HES}_{i,t} + \epsilon^{CHP-HP}_{i,t}) = H_{i,t} + H^{CHP}_{i,t} + H^{HP}_{i,t} \tag{30}$$

$$T^{SHN}_{r,i,t} + \epsilon^{HES}_{i,t} + \epsilon^{CHP-HP}_{i,t} = T^{SHN}_{s,i,t} \tag{31}$$

where $\epsilon^{HES}_{i,t}$ and $\epsilon^{CHP-HP}_{i,t}$ are thermal potentials reflecting temperature increasing of SHN fluids. $T^{SHN}_{s,i,t}$ and $T^{SHN}_{r,i,t}$ denote the supply and return temperature of the radiator, respectively. $R^{HES}_{i,t}$ and $R^{RAD}_{i,t}$ are the thermal resistance of the HES and radiator, and can be represented as a function of the mass flow rates that enter them, $\dot{m}^{HES}_{i,t}$ and $\dot{m}^{RAD}_{i,t}$.

$$R^{HES}_{i,t} = R\left(\dot{m}^{HES}_{i,t}, \dot{m}_i\right) \tag{32}$$

$$R^{RAD}_{i,t} = R\left(\dot{m}^{SHN}_{i,t}\right) \tag{33}$$

The detailed expression can be found in the supplementary material [14].

The total mass flow rate of SHN that enters the radiator $\dot{m}^{SHN}_{i,t}$ is a designed value determined by capacity of local pumps. Nevertheless, $\dot{m}^{HES}_{i,t}$ can be adjusted within a given range $[\underline{\dot{m}^{HES}_i}, \overline{\dot{m}^{HES}_i}]$, and (28) can be equivalently written as:

$$\underline{R^{HES}_{i,t}} H_{i,t} \le T^{PHN}_{s,i,t} - T^{SHN}_{r,i,t} \le \overline{R^{HES}_{i,t}} H_{i,t} \tag{34}$$

where $\underline{R^{HES}_{i,t}}$ and $\overline{R^{HES}_{i,t}}$ can be calculated by substituting $\overline{\dot{m}^{HES}_i}$ and $\underline{m^{HES}_i}$ into (32) respectively.

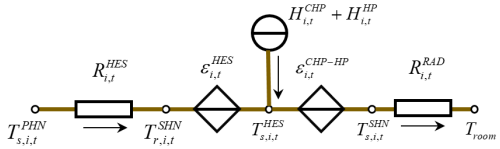

(a). SHN in HC mode

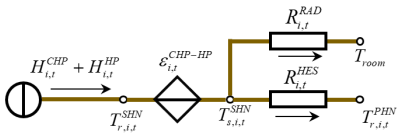

(b). SHN in HS mode

Fig. 3. Heat current model of the secondary heating network

2) Heat current model of HS nodes: Fig. 3(b) presents the heat current model of SHN in HS modes. The constraints are:

$$T^{SHN}_{s,i,t} - T^{PHN}_{r,i,t} = R^{HES}_{i,t} |H_{i,t}| \tag{35}$$

$$T^{SHN}_{s,i,t} - T_{room} = R^{RAD}_{i,t} H^l_{i,t} \tag{36}$$

$$(\dot{m}^{RAD}_{i,t} + \dot{m}^{HES}_{i,t}) c_p \epsilon^{CHP-HP}_{i,t} = H^{CHP}_{i,t} + H^{HP}_{i,t} \tag{37}$$

$$T^{SHN}_{r,i,t} + \epsilon^{CHP-HP}_{i,t} = T^{SHN}_{s,i,t} \tag{38}$$

Similar to the constraints of HC agents, (35) is replaced with:

$$\underline{R_i^{HES}}|H_{i,t}| \le T_{s,i,t}^{SHN} - T_{r,i,t}^{PHN} \le \overline{R_i^{HES}}|H_{i,t}| \quad (39)$$

The safety constraint of the supply water is:

$$T_{s,i,t}^{PHN} \le \overline{T^{PHN}} \quad (40)$$

III. Fully Decentralized Optimization of the Networked DESs

A. Optimization Problem Formulation

The optimization objective is to minimize the operational cost of all the DESs,

$$\min \sum_{i\in\mathbb{N}} \sum_{t\in\mathbb{T}} C_{i,t} \quad (41)$$

The constraints include the DN, PHN and DES operation constraints in section II. The entire formulation is a separable convex one, which can be conveniently solved through an application of ADMM [5].

B. Fully Decentralized optimization method

Denote DES i's decision variables as $\boldsymbol{X}_i$. DES i need to share a part of $\boldsymbol{X}_i$ to its neighbours for them to formulate the constraints. Specifically, in the DN, i need to share $P'_{i,t}$ and $Q'_{i,t}$ to father node A_i and $v_{i,t}$ to its child nodes $j \in \mathbf{C}_i$. In the PHN, i need to share $T_{s,i,t}^{mix}$ to its downstream nodes and $T_{r,i,t}^{mix}$ to its upstream nodes in the supply pipelines. Meanwhile, DES i needs to copy the corresponding variables shared by neighbouring nodes, which are denoted as $\boldsymbol{X}_i^j$. The copied variables should equal to the original ones, or namely, $\boldsymbol{X}_i^j = B_{i,j}\boldsymbol{X}_j$. $B_{i,j}$ is the coupling coefficient matrix.

According to ADMM, the subproblem of node i is:

$$\begin{aligned}\min_{\boldsymbol{X}_i, \boldsymbol{X}_i^j \forall j\in\mathcal{N}_i} & \sum_{t\in\mathbb{T}} C_{i,t} + \sum_{j\in\mathcal{N}_i} \frac{\rho}{2}\|\boldsymbol{X}_i^j - B_{i,j}\boldsymbol{X}_j + \frac{\boldsymbol{\lambda}_{ij}}{\rho}\|^2 \\ & + \sum_{j\in\mathcal{N}_i} \frac{\rho}{2}\|B_{j,i}\boldsymbol{X}_i - \boldsymbol{X}_j^i + \frac{\boldsymbol{\mu}_{ij}}{\rho}\|^2 \\ s.t. \quad & \boldsymbol{h}_i(\boldsymbol{X}_i, \boldsymbol{X}_i^{j_1}, \boldsymbol{X}_i^{j_2}, ...) \le \mathbf{0} \quad j_1, j_2, ... \in \mathcal{N}_i \end{aligned} \quad (42)$$

where $\boldsymbol{\lambda}$ and $\boldsymbol{\mu}$ are dual variables. $h(\cdot)$ includes all the constraints. $\mathcal{N}_i$ denotes the set of all the neighbouring nodes of DES i in DN and PHN. In the subproblem of node i, $\boldsymbol{X}_i$,$\boldsymbol{X}_i^j$ are decision variables. $B_{i,j}\boldsymbol{X}_j$ and $\boldsymbol{X}_j^i$ should be collected from neighbouring nodes and treated as boundary conditions.

The decentralized scheme is described in algorithm 1. In the proposed method, each DES exchanges local information and makes decisions equally. When all the subproblems have converged, the iteration terminates.

IV. Case Study

A. System Description

The topology of the test system consisting of a IEEE 14-node DN and a 14-node PHN is shown in Fig.4. Node with same labels represent the same DES, and in total 17 DES agents participate in the decentralized dispatch. The red arrows define the flow direction in PHN supply pipelines. Node 5 and 11 of the PHN are in HS modes and the other nodes are in HC modes. The switching of DES between these modes are not considered, because this is related to hydraulic status of the PHN and hard to realize in engineering practices. The detailed load distribution, the capacities of devices in each DES, and the PHN information are disclosed online in [14]. The dispatch interval is one hour. All of the optimization problem are solved with solver ECOS [15] on a PC with 3.2GHz CPU.

Algorithm 1 Optimization process for each DES i

1: Collect $B_{i,j}\boldsymbol{X}_j$ and $\boldsymbol{X}_j^i$ from each neighbouring RES node j in DN and PHN.
2: Update the dual variables stored at i through $\boldsymbol{\lambda}_{ij} := -\boldsymbol{\mu}_{ji}$, $\boldsymbol{\mu}_{ij} := -\boldsymbol{\lambda}_{ji}$
3: Solve the subproblem (42)
4: Update the dual variables
$\boldsymbol{\lambda}_{ij} := \boldsymbol{\lambda}_{ij} + \rho\left(\boldsymbol{X}_i^j - B_{i,j}\boldsymbol{X}_j\right)$,
$\boldsymbol{\mu}_{ij} := \boldsymbol{\mu}_{ij} + \rho\left(B_{j,i}\boldsymbol{X}_i - \boldsymbol{X}_j^i\right)$,
5: Calculate the primal and dual residuals
$R_{p,i} = \|[\boldsymbol{X}_i^j - B_{i,j}\boldsymbol{X}_j, B_{j,i}\boldsymbol{X}_i - \boldsymbol{X}_j^i\|_\infty$
$R_{d,i} = \|\boldsymbol{X}_i - \boldsymbol{X}_i^{last}\|_\infty$ and check the convergence with threshold = 10^{-3}. If the subproblem has not converged, broadcast updating signals and return to step 1.

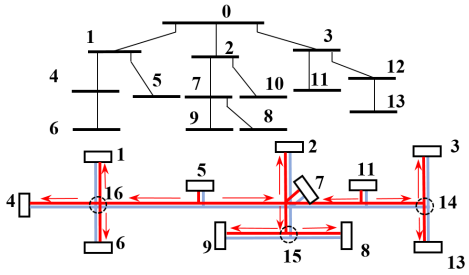

Fig. 4. The topology of the test system

B. Results and Discussion

The convergence trajectories of the decentralized optimization is given in Fig.5. The objective function value reaches \$71402.9 and the primal and dual residuals reach 10^{-3} in 2000 iterations. Each iteration of each agent takes 0.02s on average, which is acceptable for parallel calculation. Another test on a 44 node system also indicates the scability in larger systems. Details can be found in [14].

To verify the correctness and effectiveness of the proposed method and model, the result is compared to those of a centralized optimization approach where commercial solvers are directly employed. Two different models are considered. In the first model, all constraints are included, and in the second one, the heat transfer constraints (28)-(31) and (35)-(38) are dismissed. Note that in the latter model, the optimization problem is not well-posed because there are no active lower bounds on the supply water temperature, which may lead to results inconsistent to physical laws. Therefore, the following constraint without much physical interpretability is presented as a supplement [9].

$$T_{s,i,t}^{PHN} \ge \underline{T^{PHN}} \quad (43)$$

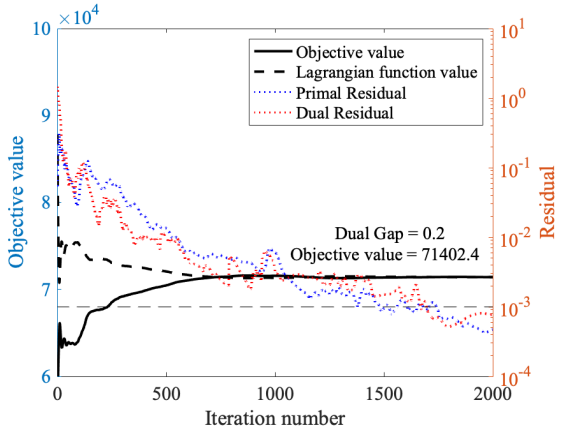

Fig. 5. Iteration curves of the optimization objective

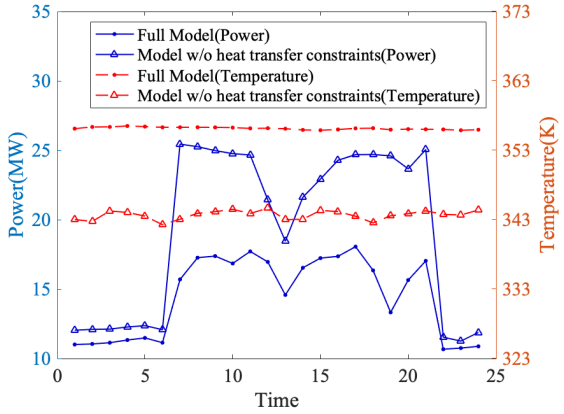

Fig. 6. Heat exchange of HC nodes with PHN and average supply water temperature

The operation costs are compared in Table I. The result obtained by the centralized approach using the full model is close to that of decentralized dispatch, which means the proposed model can be properly solved through ADMM. However, when heat transfer constraints are omitted, the result turns out remarkably lower. Fig. 6 compares the heat exchange of HC nodes with the PHN and average supply water temperature. Compared to the full model, the heat extraction without heat transfer constraints is higher and supply water temperature is lower. This is because end users have unrestricted access to heat in the PHN regardless of water temperature and delay, which results in unreasonable low costs.

V. Conclusion

In this work, we model the multiple DESs with interconnected power distribution and heating systems. The delay and loss characteristics are considered and the heat transfer constraints of the heating network are modelled through the heat current method. A fully decentralized optimization scheme is employed to solve the dispatch problem. The case study on a system with in total 17 DES agents demonstrates the effectiveness of the method and significance of a comprehensive modelling of the heating system. Note that in this work the PHN is operated at "quality regulation" mode where mass flow rates which are pre-given numbers. In our future work, we will focus on a more effective decentralized optimization scheme considering both quality and quantity control of heating networks and loads and RES uncertainties in multi-energy systems, where heating networks can be better exploited to promote RES accommodation.

TABLE I
Comparisons of results between different Models

	Full model	No heat transfer constraints
cost($)	71402.4	68923.7(-3.47%)

References

[1] L. Li, X. Cao, and P. Wang, "Optimal coordination strategy for multiple distributed energy systems considering supply, demand, and price uncertainties," *Energy*, vol. 227, p. 120460, 2021.

[2] C. Wei, Z. Shen, D. Xiao, L. Wang, X. Bai, and H. Chen, "An optimal scheduling strategy for peer-to-peer trading in interconnected microgrids based on ro and nash bargaining," *Applied Energy*, vol. 295, p. 117024, 2021.

[3] D. K. Molzahn, F. Dörfler, H. Sandberg, S. H. Low, S. Chakrabarti, R. Baldick, and J. Lavaei, "A survey of distributed optimization and control algorithms for electric power systems," *IEEE Trans. Smart Grid*, vol. 8, no. 6, pp. 2941–2962, 2017.

[4] Z. Yang, R. Wu, J. Yang, K. Long, and P. You, "Economical operation of microgrid with various devices via distributed optimization," *IEEE Trans. Smart Grid*, vol. 7, no. 2, pp. 857–867, 2016.

[5] S. Boyd, N. Parikh, E. Chu, B. Peleato, and J. Eckstein, *Distributed Optimization and Statistical Learning via the Alternating Direction Method of Multipliers*. Now Publishers Inc., 2011.

[6] A. Rabiee, B. Mohammadi-Ivatloo, and M. Moradi-Dalvand, "Fast dynamic economic power dispatch problems solution via optimality condition decomposition," *IEEE Trans. Power Syst.*, vol. 29, no. 2, pp. 982–983, 2014.

[7] C. Lin, W. Wu, B. Zhang, and Y. Sun, "Decentralized solution for combined heat and power dispatch through benders decomposition," *IEEE Trans. Sustain. Energy*, vol. 8, no. 4, pp. 1361–1372, 2017.

[8] Y. Cao, W. Wei, L. Wu, S. Mei, M. Shahidehpour, and Z. Li, "Decentralized operation of interdependent power distribution network and district heating network: A market-driven approach," *IEEE Trans. Smart Grid*, vol. 10, no. 5, pp. 5374–5385, 2019.

[9] D. Xu, Q. Wu, B. Zhou, C. Li, L. Bai, and S. Huang, "Distributed multi-energy operation of coupled electricity, heating, and natural gas networks," *IEEE Trans. Sustain. Energy*, vol. 11, no. 4, pp. 2457–2469, 2020.

[10] H. Zhu, T. Yu, Z. Chen, Y. Wu, Z. Li, and W. Wu, "Distributed optimal dispatching of interconnected electricity-gas-heating system," *IEEE Access*, vol. 8, pp. 93 309–93 321, 2020.

[11] K.-L. He, Q. Chen, H. Ma, T. Zhao, and J.-H. Hao, "An isomorphic multi-energy flow modeling for integrated power and thermal system considering nonlinear heat transfer constraint," *Energy*, vol. 211, p. 119003, 2020.

[12] J. Hao, Q. Chen, K. He, L. Chen, Y. Dai, F. Xu, and Y. Min, "A heat current model for heat transfer/storage systems and its application in integrated analysis and optimization with power systems," *IEEE Trans. Sustain. Energy*, vol. 11, no. 1, pp. 175–184, 2020.

[13] M. Farivar and S. H. Low, "Branch flow model: Relaxations and convexification—part i," *IEEE Trans. Power Syst.*, vol. 28, no. 3, pp. 2554–2564, 2013.

[14] "Supplementary Materials and Test Data," 2022. [Online]. Available: "https://github.com/falcon-sqh/TSG-dec_robust_dispatch"

[15] A. Domahidi, E. Chu, and S. Boyd, "Ecos: An socp solver for embedded systems," in *2013 European Control Conference*, 2013, pp. 3071–3076.